REPORT ON LACE STAY AT CHMI, PRAGUE,
18th July - 19th August 2022.

# Further sensitivity studies with radar reflectivity data assimilation

*Suzana Panežić*

*Meteorological and Hydrological Service, Croatia*

In collaboration with Alena Trojáková and Antonín Bučánek
(CHMI, Czech Republic)

13/12/2022

# 1 Introduction

During the 2012-2018 period, a lot of European countries have invested into upgrading their weather radars, which led to increased quality of the incoming data [1]. With increasing need to improve forecast of the extreme precipitation episodes, priority to assimilate such data into the regional NWP models has been put into RC LACE development plans.

Within the scope of ALARO CSC, Trojáková [5] has investigated the usage of radar reflectivity observation operator and Bučánek [4] has worked on increased understanding of the 1D Bayesian retrieval of pseudo observed relative humidity as was originally proposed by Wattrelot [3] for the AROME CSC (concept by Caumont [2]). With several RC LACE member countries reporting the drying effect during the radar reflectivity data assimilation evaluation, an impact study has been performed by Panežić, Trojáková and Bučánek [6] which showed enhanced impact of dry observation on the analysis, causing the drying of the atmosphere. Two solutions have been proposed by Strajnar [7] and Bučánek [8].

The aim of this study is to evaluate the impact of the two proposed solutions. Specific focus has been put on definition of the radar minimal detectable reflectivity factor.

# 2 Treatment of dry observations

## 2.1 Minimal detectable reflectivity factor

Radars operate by emitting an electromagnetic signal and detecting an echo reflected off the objects. The nature of the echo signal provides information about the object itself. Received signal contains noise and signal distortions that need to be removed before using this type of data. In meteorological radars, the object of interest are precipitating systems so, during signal and data processing phase, undesired signals are rejected or removed (such as land/sea clutter and aircrafts) and signals describing detected hydrometeors are kept [9].

Radar reflectivity can be defined as a sum of all backscattering crossections (precipitation particles) in a pulse resolution volume divided by that volume. For data assimilation purposes in the NWP model ALADIN we distinguish between two types of reflectivity data. First type are reflectivity data that are actually measured and are denoted here as wet observations (flgdyn=8). Second type are undetected reflectivity data (no-rain information), which happen when returned signal is below the detection threshold of the radar. As shown by Watterlot [3] we need the minimum detectable reflectivity factor (MDRF) to properly assimilate such no-rain information. The radar sensitivity or detection threshold (zthreshold in code) can be expressed as a function of distance from radar $r$ as follows:

$$zthreshold(r) = MDRF + 20log_{10}(r) \tag{1}$$

where MDRF is the value of the minimum detectable reflectivity factor at distance of 1km from the radar. In reality, MDRF varies slightly from radar to radar due to different tower heights, anntena gain, coupled losses, etc. The MDRF is by default calculated by BATOR from the radar reflectivity data and all undetected reflectivity data are set to equal the detection threshold values by BATOR (flgdyn=0). These values are applied only to dry observations, while wet ones remain as they are measured. As each radar scan is different, in practice, BATOR

calculated MDRF value varies considerably between each volume scan, as seen in Figure 1 (blue dots). It is questionable if this feature of BATOR is desirable.

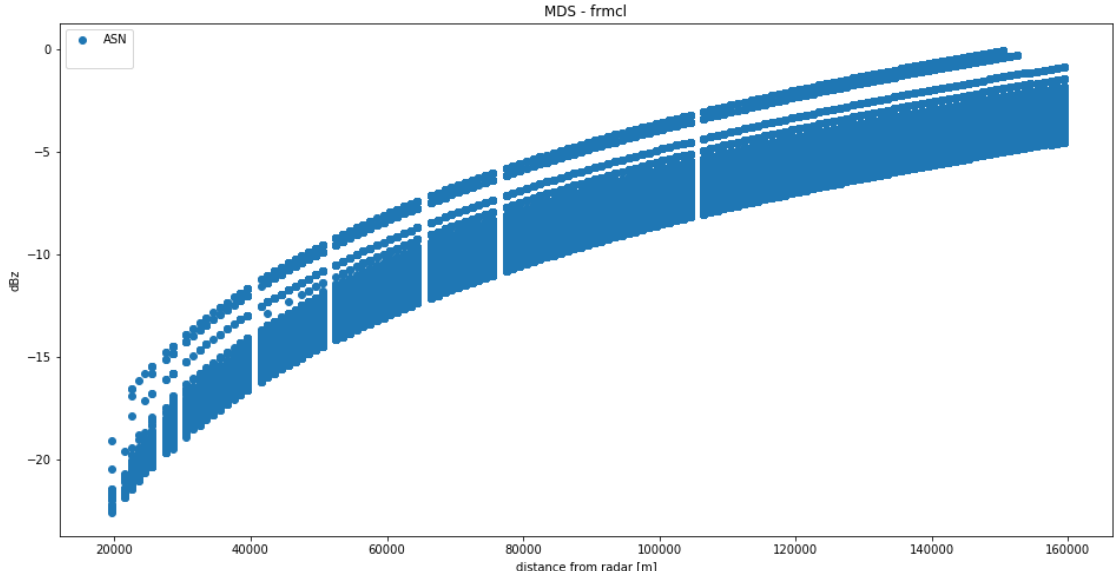


Figure 1: Detection threshold values for radar Montclar (frmcl) for period 20.-23.06.2022 calculated by BATOR.

## 2.2 MF BATOR code modification

Since Météo France (MF) cy43t2_op3 code version, a modification to BATOR code that removes all dry observations where the value of BATOR detection threshold exceeds zero value was introduced. This means that the noise has exceeded the signal level and it is no longer assured that the dry observation is truly a non-rainy pixel. As such it is no longer sensible to use such observations in the data assimilation (communication with Maud Martet). In practice, this reduces the radius size (distance from the radar) within which the dry observations are used, as shown in the example of Slovenian radar Lisca (silis) on Figure 2.

**Modified sources:**

`Odb/pandor/module/bator_decodhdf5_mod.F90`

## 2.3 Proposed solution by Bučánek

To mitigate the drying effect observed during radar data assimilation Bučánek proposed two modifications. Firstly, MDRF values are set to a constant per radar site to avoid large variation of BATOR computed values. The BATOR algorithm for computation of MDRF values struggles when no or very little rain is observed by radar. New constant MDRF values are computed offline by the same algorithm as in BATOR but over a longer rainy period. Changes of MDRF values with elevation are neglected in this approach. In order to compensate for this

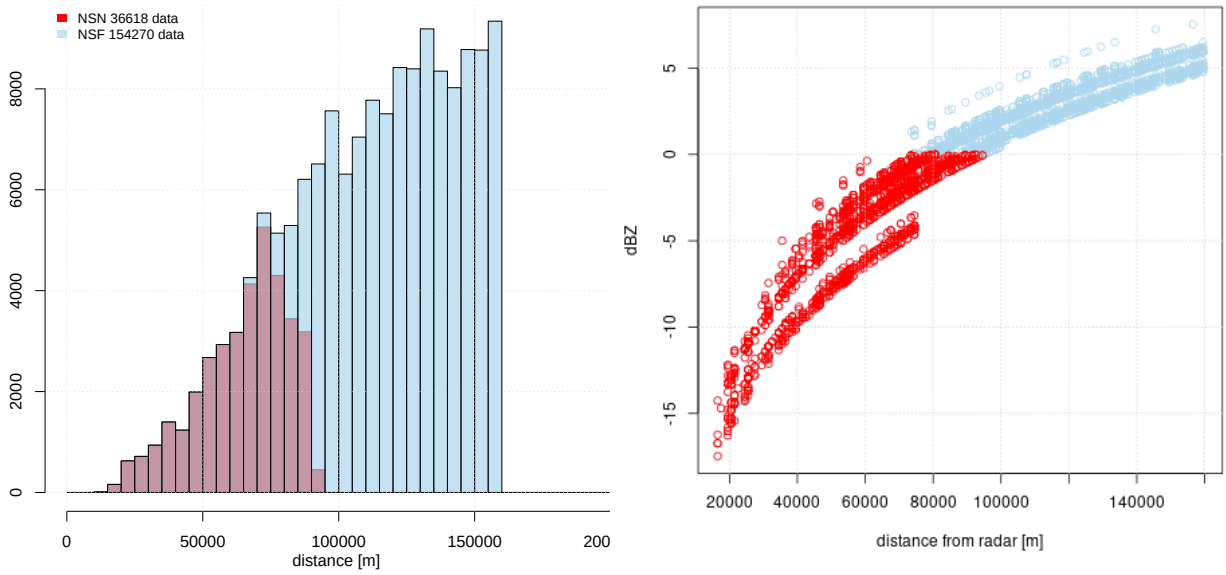


Figure 2: Dry observation count (left) and detection threshold values (right) - radar silis for period 20. - 30.06.2022 without MF BATOR code modification (blue) and with MF BATOR code modification (red).

simplification and for possible inaccuracies in model observation operator the offset of +10dBZ is used:

$$zthreshold(r) = MDRF + 20log_{10}(r) + offset \tag{2}$$

During OPERA files preprocessing, new MDRF values are written to radar files through the HOOF namelist and later read by BATOR. Example of the new detection threshold values as opposed to the BATOR calculated ones can be seen on Figure 3 for the Czech radar Brdy (czbrd).

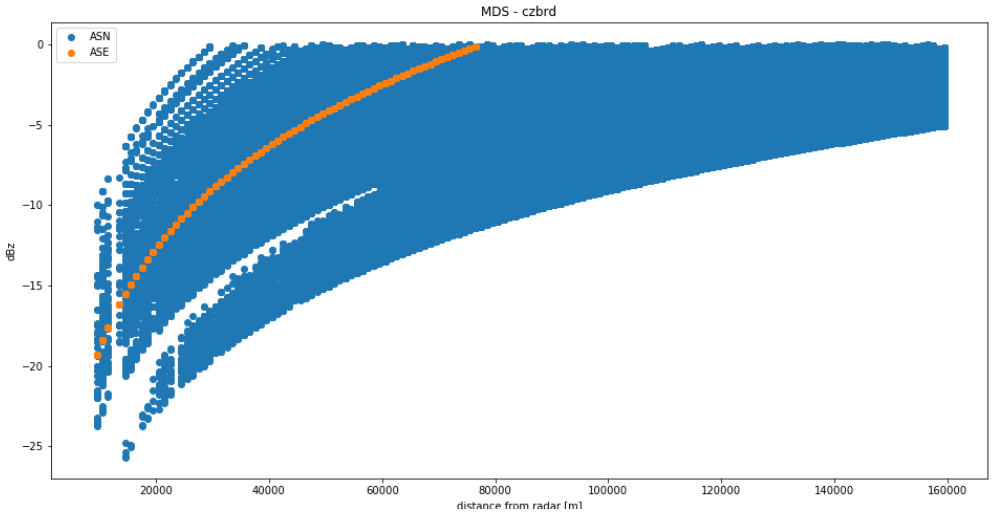


Figure 3: Detection threshold values - radar czbrd for period 20.06.2022 - 01.07.2022 calculated by BATOR (blue), predefined using constant MDRF (orange).

Second modification consists of removing all dry observations which are moistening the atmosphere. The idea is: radar didn't detect any reflectivity at the location (undetect value) and the model sets the value to the radar detection threshold there. It could be seen as an upper bound for real reflectivity in the atmosphere in that location. If the model reflectivity is lower than this upper bound it should be ignored since we do not know anything about real values and those could be anywhere between upper bound and minus infinity (personal communication with Antonín Bučánek).

**Modified sources:**

```
Odb/pandor/module/bator_module.F90
Odb/pandor/module/bator_decodhdf5_mod.F90
Arp/op_obs/obsop_radar.F90
Arp/op_obs/hdepart.F90
```

### 2.4 Proposed solution by Strajnar

Another approach to mitigate the drying effect was proposed by Strajnar. This concept consists of assimilating only observation places where considerable precipitation is either forecasted or observed (i.e. model or observation reflectivity factor is above 12 dBZ).

**Modified sources:**

```
Arp/op_obs/inv_refl1dstat.F90
```

## 3 Model setup specification

All experiments used the ALARO/CZ operational configuration with recently implemented prognostic graupels. Effect of prognostic graupels on the radar reflectivity observation operator itself was not investigated.

- Model: ALARO NH-v1B cy43t2ag_op1
- Domain: ALARO/CZ; $\Delta x = 2.3$ km; 1069x853 GP; 87 vertical levels; mean orography,
- Coupling: 3h space consistent coupling from ARPEGE; synchronous
- Upper air analysis: BlendVar scheme (DF blending, filtering at truncation E102x81) followed by 3D-Var; 6h Assimilation cycle; REDNMC=0.5, Ensemble data assimilation B matrix based on AEARP;
- Assimilated observation: SYNOP, TEMP, AMDAR, SEVIRI, Mode-S MRAR/Mode-S EHS, HR-AMV, wind profiler, ASCAT.

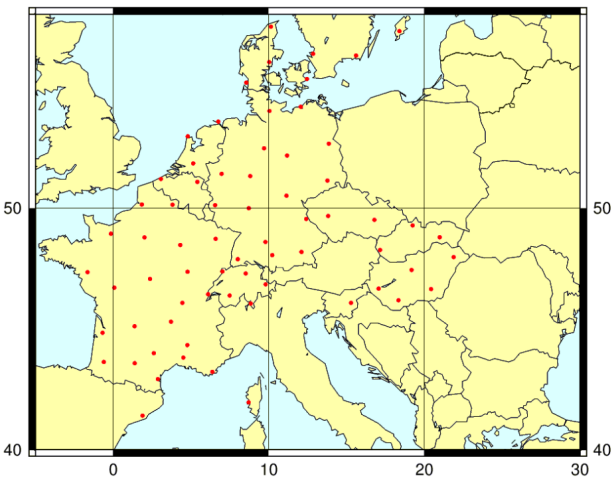


Figure 4: Radars used in the experiments

Reflectivity radar data were provided by the OPERA Internet File Server (OIFS) and were processed by the Homogenization Of Opera Files (HOOF) tool, version 1.9. The option of no data splitting was used for the processing of OPERA data with HOOF.

An overview of assimilated radars (not rejected by BATOR) can be found in Figure 4. The data from Romania were not used as uncorrected reflectivity (TH) is not available and data from Poland have zero total quality flags.

Following previous study by Panežić et al. [6] the radar data assimilation was set to use the model profile selection box size of 100km and the reflectivity observation error $\sigma = 0.2$. Experiments were carried out over the period 20.6.2022 - 30.6.2022 containing several extreme precipitation events in the Czech Republic. As impact of data assimilation in LAM is usually prominent in the forecast up to 6 -12 hours, only 6 hourly data assimilation cycle was performed and evaluated.

All code modifications regarding proposed solutions and additional experiments were merged into a single pack under separate logical keys and values that can be called or defined though the BATOR and SCREENING namelists. One error in code was found in Bučánek solution during this phase and was corrected.

**New BATOR related logical keys and variables:**

- LREADMDS - reads constant MDRF values added by HOOF and applies attenuation correction for non-french radars; otherwise calculates MDRF values from input data
- LREADMDSMOD - hardcoded elevation dependant MDRF values for German and Czech radars; otherwise uses single constant MDRF value for German and Czech radars (this part should be removed from the code as it contaminates other MDRF reading/calculating options but is relevant for a few experiments in this report)
- LNOISEDISTRED - MF modification; removes all dry observations where detection threshold values exceed some value (connected with ZNULTHRVAL variable); otherwise all dry observation values up to 160 km distance from radar are used
- ZRADOFFSET - variable which defines offset values applied then calculating the detection threshold (default is ZRADOFFSET=0)
- ZNULTHRVAL - variable which defines a dry observation cut off value (connected with LNOISEDISTRED logical key; default is ZNULTHRVAL=0)

**New SCREENING related logical keys and variables:**

- LRAINTHR - removes all observation places where no considerable precipitation is either forecasted or observed; otherwise uses default conditions on negative observation and simulation
- LRMDRYOBSMOIST - removes all dry observations which have a moistening effect; otherwise keeps them
- LMAXHEIGHT10KM - removes all observations above the 10 km altitude; otherwise keeps them
- ZRAINTHRVAL - variable which defines the threshold values related to LRAINTHR logical key; default is ZRAINTHRVAL=12

# 4 Results and discussion

In order to differentiate and evaluate the impact of the specific modifications, numerous experiments were set up. Summary of the used keys in different experiments can be found in Appendix A (BATOR modifications) and Appendix B (DA modifications).

## 4.1 Evaluation of MF BATOR code modification

In order to differentiate the impact of MF BATOR code modification, separate experiment was set up (named NSN for passive and ASN for active radar data assimilation). It was compared to default experiment used during last stay with no additional code modifications (NSF/ASF).

- NSF - passive radar DA exp with default MDRF computation
- NSN - as NSF but with MF BATOR code modifications (no dry data above 0dBZ)
- ASF - active radar DA exp with default MDRF computation
- ASN - as ASF but with MF BATOR code modifications (no dry data above 0dBZ)

Results were evaluated for both passive and active experiments of all available observations (Figure 5). Departures statistics of simulated reflectivity, pseudo-observed relative humidity and pseudo-observed reflectivity derived by the 1D Bayesian inversion (ODB statistics hereafter) showed decreased counts of dry observations, a larger reflectivity bias but a smaller dry pseudo-observed RH bias in NSN/ASN experiments which might be explained by removed dry observations where the value of detection threshold exceeds zero value.

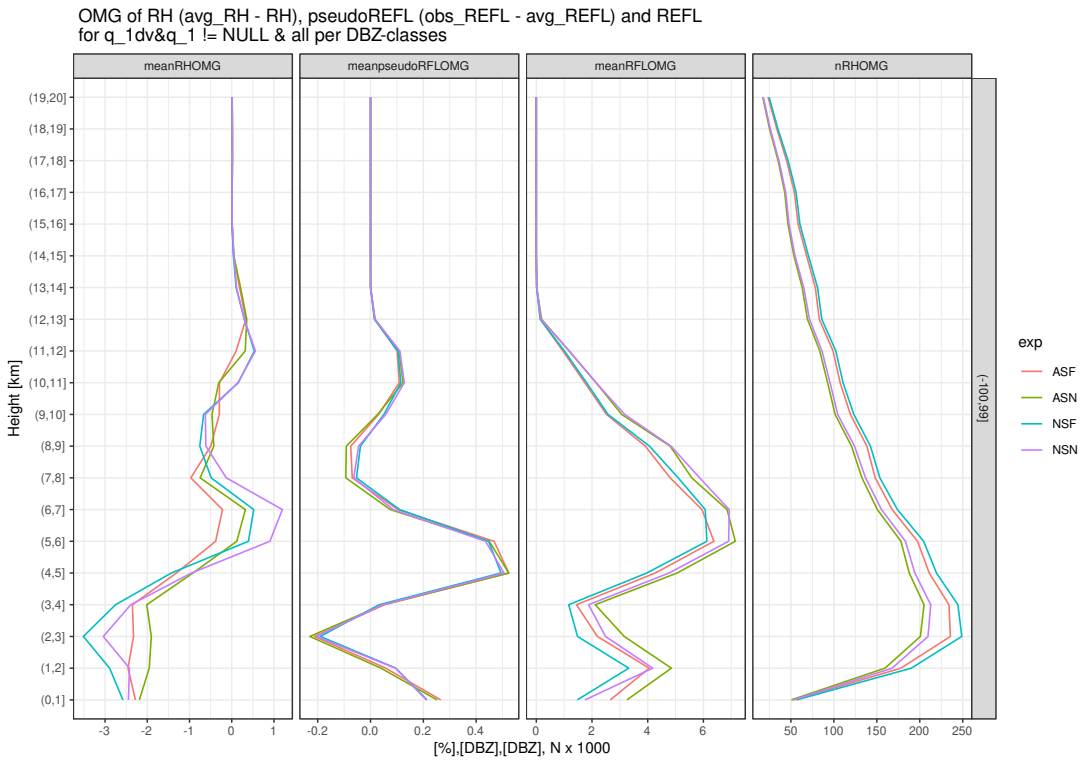


Figure 5: BIAS of departures for pseudo-observed RH, pseudo-observed reflectivity and simulated reflectivity and their count for all observations in ASF, ASN, NSF, and NSN experiments

The signal is qualitatively the same but less pronounced in the active experiments (due to feedback in cycled guess which is influenced by active radar data assimilation). The conclusions hold even when only active observations are considered in the ODB statistics (Figure 6). The ODB statistics using only active data will be used in the further text.

Impact of this modification on upper-air scores was rather neutral (Figure 7) and a slightly smaller dry bias and RMSE is observed in cloudiness scores (Figure 8) for ASN compared to ASF. However both radar experiments have a large dry bias compared to the no radar data reference (AOP).

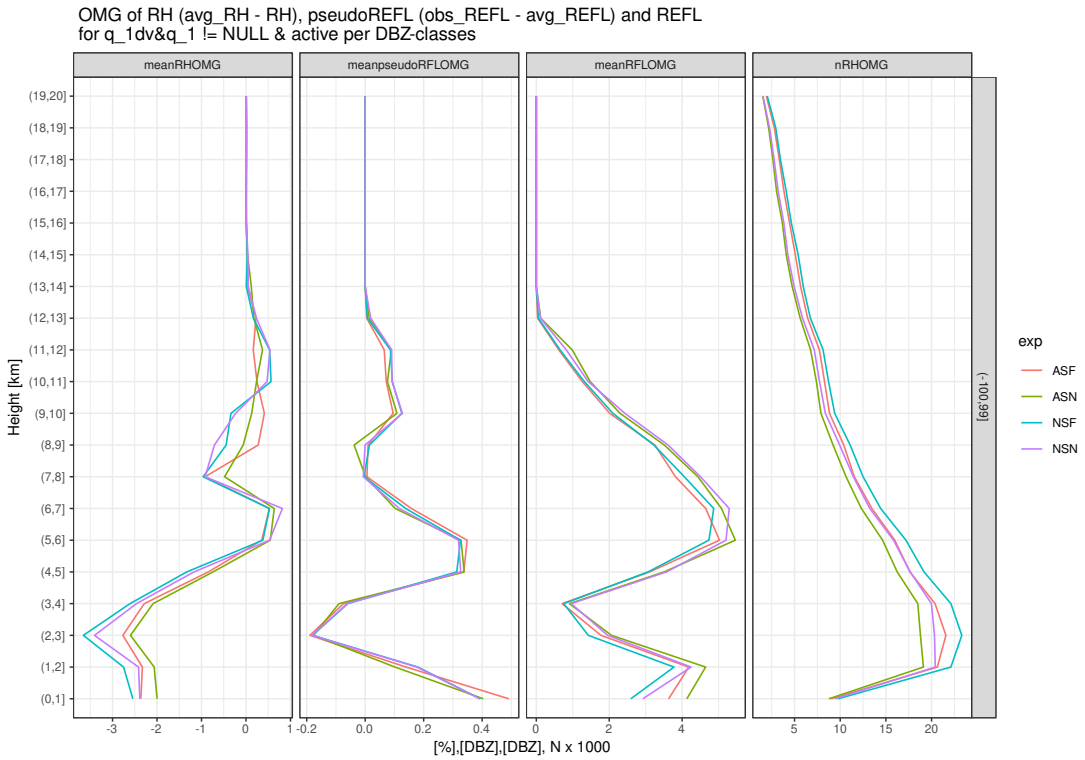


Figure 6: BIAS of departures for pseudo-observed RH, pseudo-observed reflectivity and simulated reflectivity and their count for active observations in ASF, ASN, NSF, NSN experiments

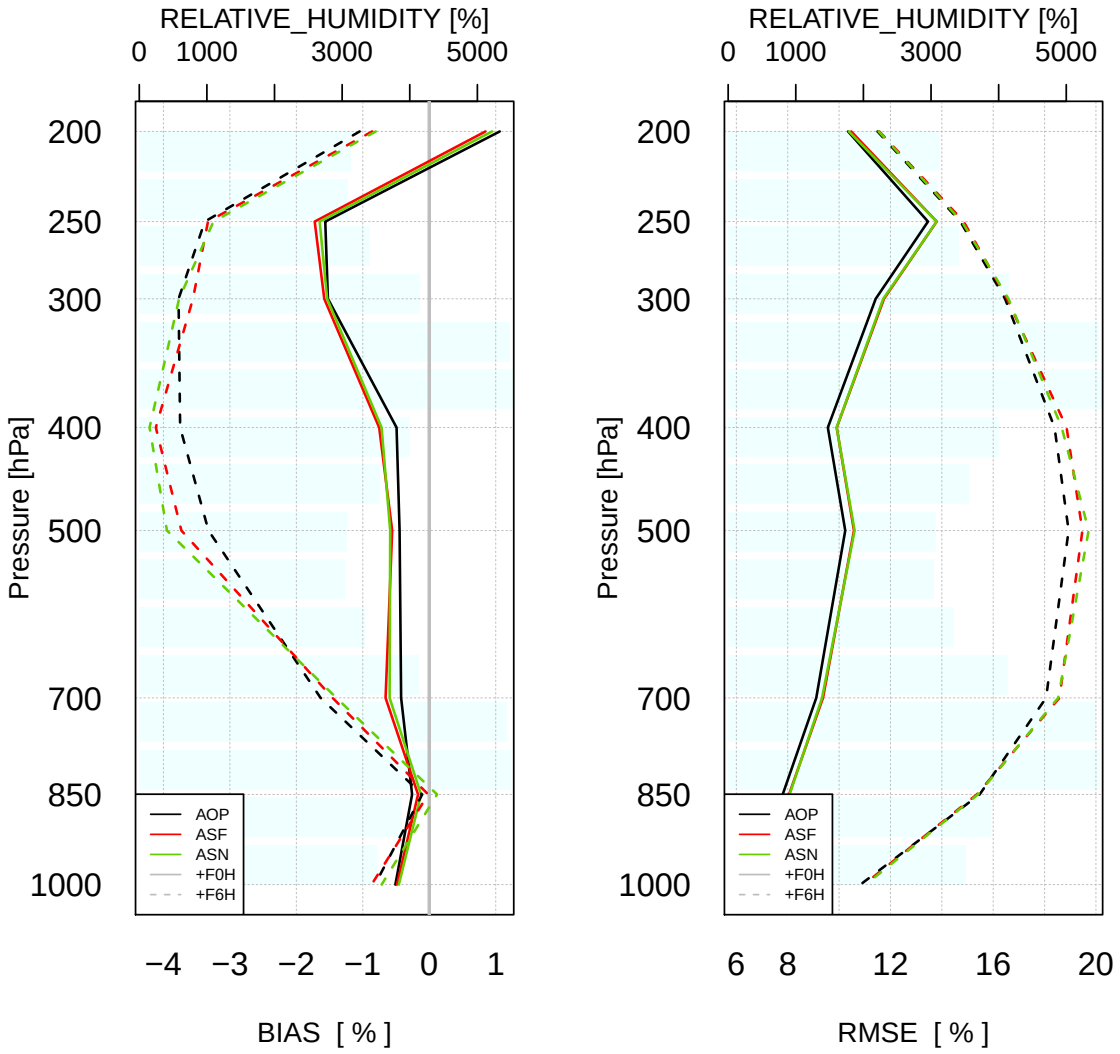


Figure 7: BIAS (left) and RMSE (right) of relative humidity for reference experiment AOP and radar experiments ASF and ASN over the assimilation period of 20-30 June 2022 for all network times (00, 06, 12 and 18 UTC).

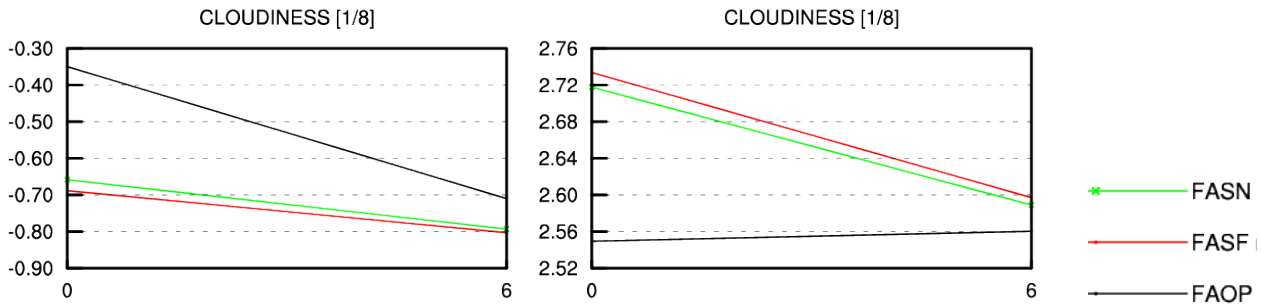


Figure 8: BIAS (left) and RMSE (right) of the cloudiness for reference experiment AOP and radar experiments ASF and ASN over the assimilation period of 20-30 June 2022 for all network times (00, 06, 12 and 18 UTC).

## 4.2 Evaluation of Bučánek solution

The impact of both modifications in Bučánek solution was evaluated as well. The experiment with only BATOR modifications (fixed value of MDRF per radar; named ASE) was compared to a full solution one (fixed value of MDRF per radar + no moistening by dry observations; named AST).

- AOP - reference without radar DA
- ASN - active radar DA with default MDRF computation & MF BATOR code modif.
- ASE - active radar DA with constant MDRF per radar & MF BATOR code modifications
- AST - as ASE + no moistening by dry observations
- AHT - as AST but removed all dry observations above 10km

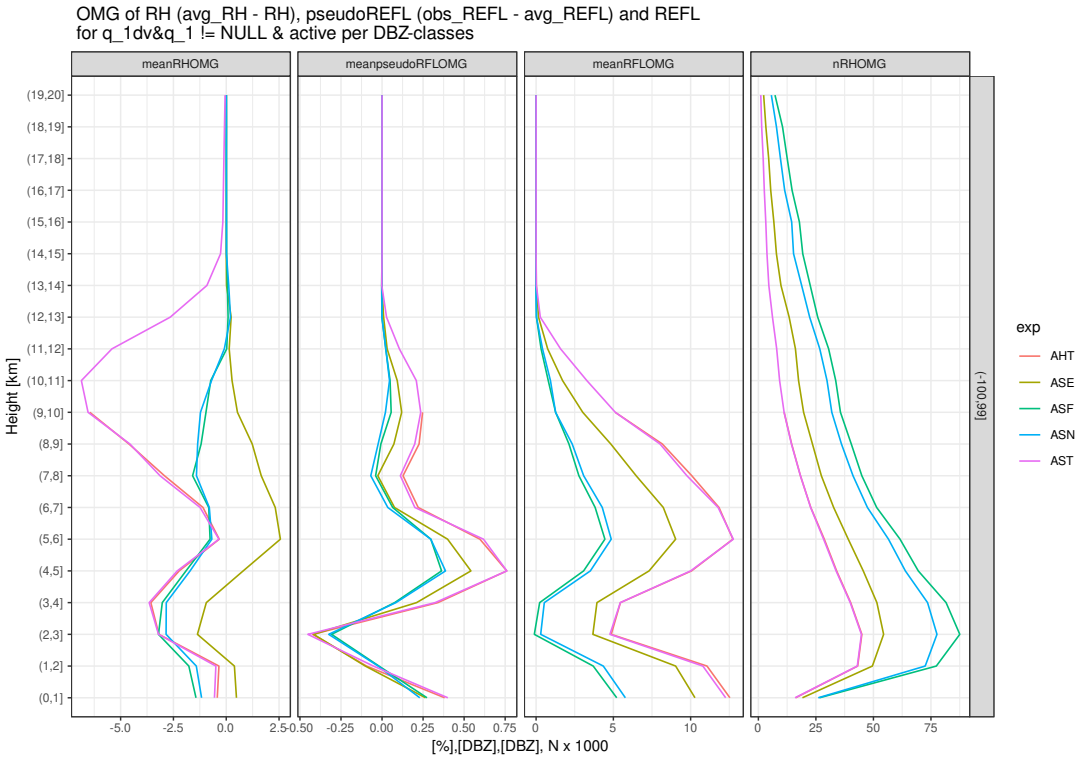


Figure 9: BIAS of departures for pseudo-observed RH, pseudo-observed reflectivity and simulated reflectivity and number of departures for ASF, ASN, ASE, AST, and ATH experiments

What could immediately be seen on ODB statistics was prominent drying of the upper atmosphere in AST experiment, as shown in Figure 9. It is also visible in verification scores on both RMSE and BIAS of upper-air relative humidity (Figure 10) and cloudiness (Figure 11).

Looking at the AST scores, the drying effect is the most prominent above 300 hPa. If the amount of data is shown on the same plot, separating dry and moist observations, it can be seen that between 400 and 200 hPa the amount of moist observations reduces quickly and above 200 hPa they are nonexistent (Figure 12). With the code modification which removes dry observations that are moistening the atmosphere (model dryer then the observation), atmosphere above 200 hPa experiences only drying. This, in turn, causes additional drying effect in the verification scores.

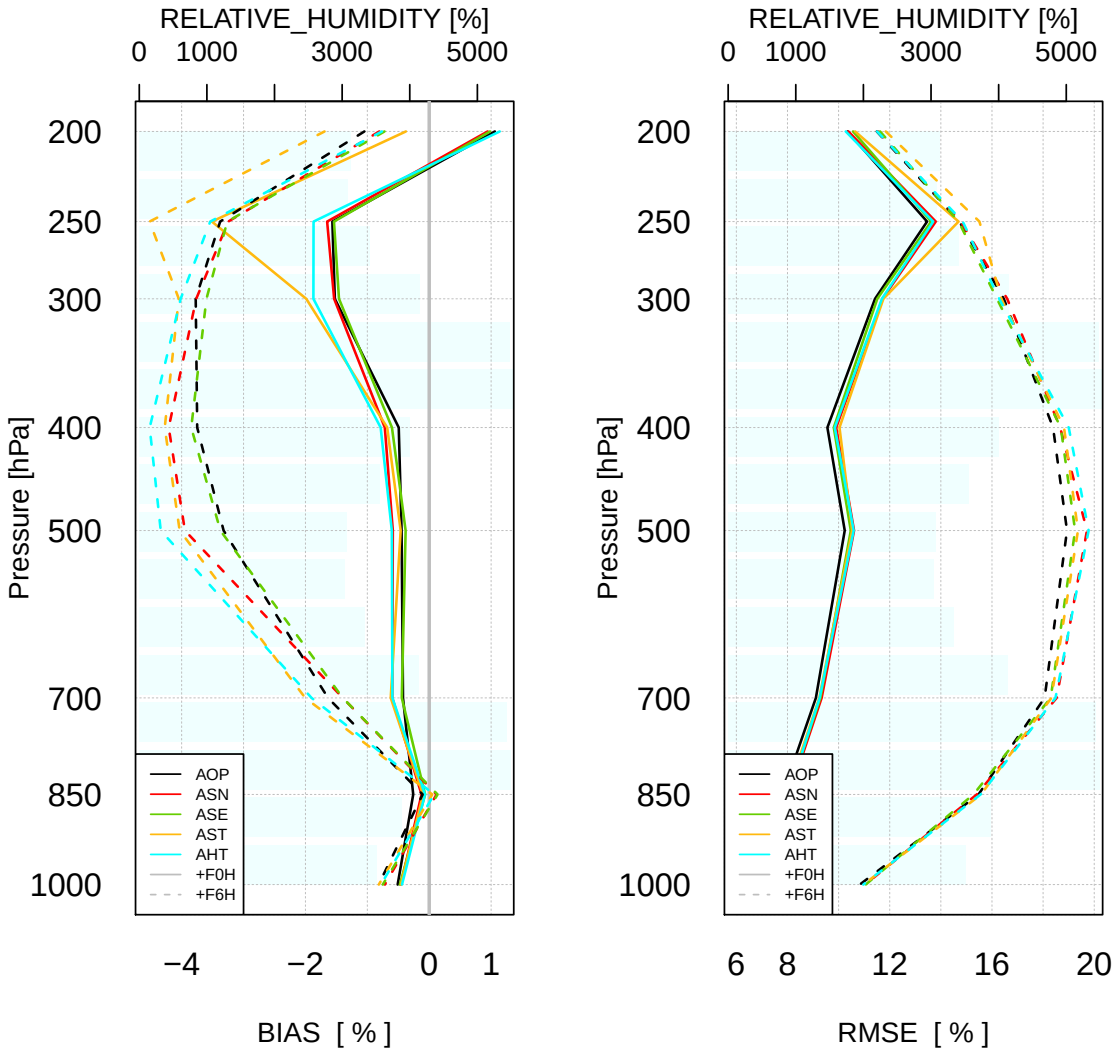


Figure 10: BIAS (left) and RMSE (right) of relative humidity for reference experiment AOP and radar experiments ASN, ASE, AST and AHT over the assimilation period of 20-30 June 2022 for all network times (00, 06, 12 and 18 UTC).

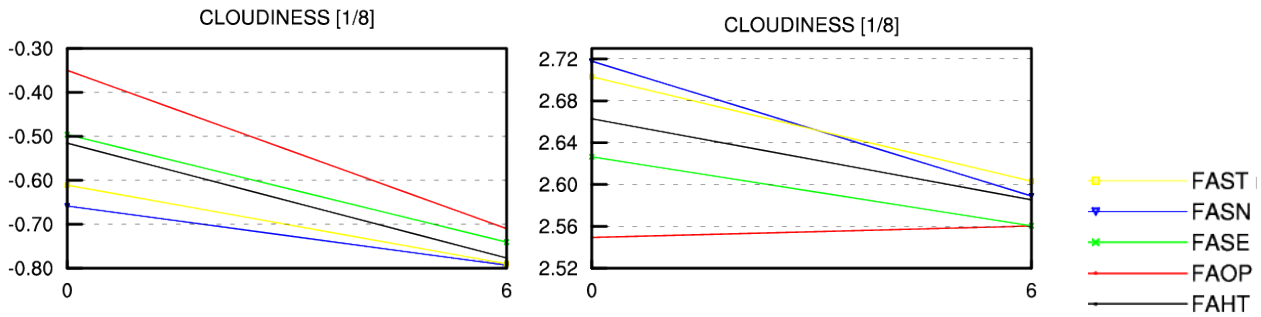


Figure 11: BIAS (left) and RMSE (right) of the cloudiness for reference experiment AOP and radar experiments ASN, ASE, AST and AHT over the assimilation period of 20-30 June 2022 for all network times (00, 06, 12 and 18 UTC).

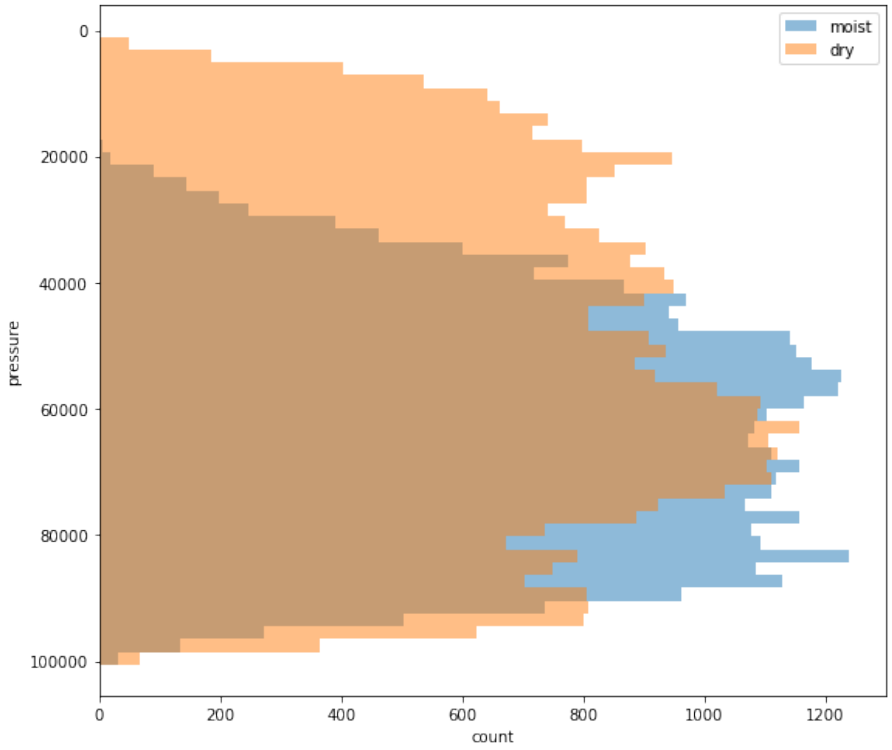


Figure 12: 2D histogram of dry (orange) and moist (blue) observations: count by height for experiment AST.

In attempt to try and mitigate this problem, additional experiment was set up, named AHT. This experiment removes all dry observations above the height of 10 km, on top of all modifications present in AST experiment. As shown in Figure 10, this modification successfully removes the increased drying above 300 hPa, but in turn degrades the 6h forecast of relative humidity in the entire vertical column towards drying of the atmosphere. This degradation is probably caused by screening preferring profiles that are more populated during the thinning phase. By removing dry data above 10 km, we are essentially depopulating profiles and different, non-optimal ones might be chosen, causing the forecast degradation. Example of differently chosen profiles between AST and AHT experiments can be seen on Figure 13. Figure shows moist observations (flgdyn=8; purple markings) and dry observation (flgdyn=0; blue markings) selected for the same analysis (20.06.2022 06 UTC run) between 680 and 700 hPa for AST (left) and AHT (right) experiments. It is clear that some profiles chosen in AST experiment were replaced by different ones during the screening process in AHT experiment.

Looking at the ASE experiment, it can be seen that there is a large sensitivity to the dry observation values. In the ODB statistics (Figure 9), it can be seen decreased counts of dry observations (probably caused by the combination of constant MDRF per radar and MF BATOR code modification), a larger reflectivity bias but the pseudo-observed RH bias doesn't exhibit the drying effect. In verification scores of upper-air relative humidity (Figure 10), it can be seen that RMSE and bias are comparable to the reference AOP, as opposed to the drying effect in all other experiments. The verification of cloudiness (Figure 11) also indicates a positive

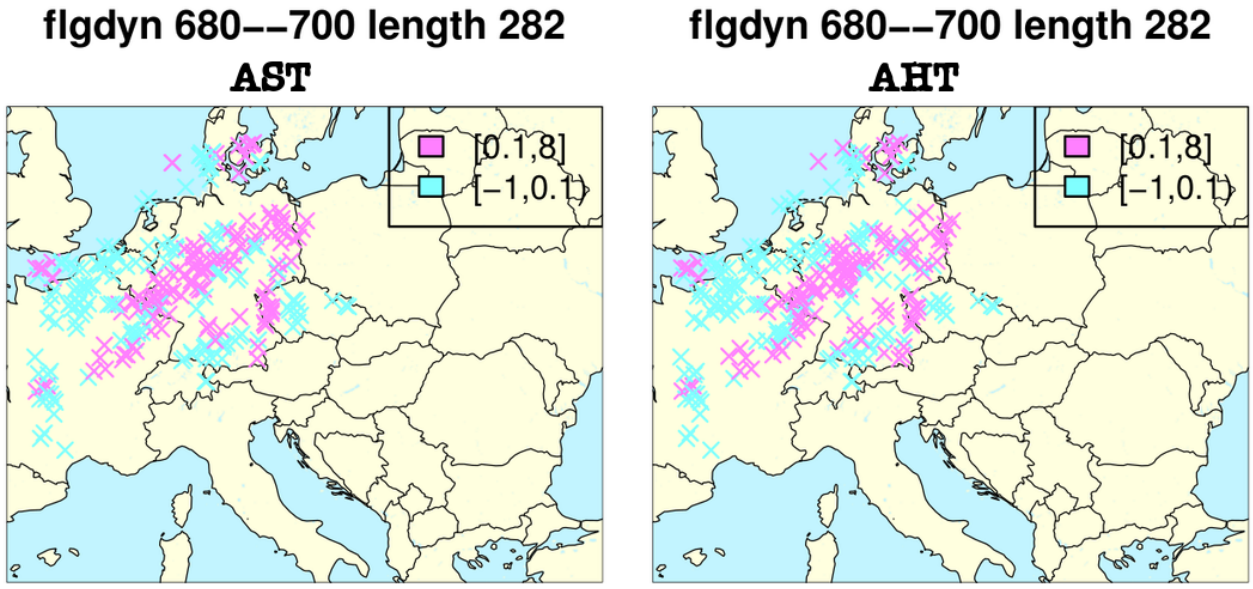


Figure 13: Screening profile selection for 20.06.2022 06 UTC analysis; vertical height between 680 and 700 hPa; experiments AST(left) and AHT(right); moist observations (purple), dry observations (blue).

impact of a constant MDRF value per radar on reduction (but not complete elimination) of the drying observed when radar data are assimilated.

The 6h precipitation scores (Figure 14) show an improved bias for all radar experiments compared to the reference without radars but at the cost of a larger RMSE/STD.

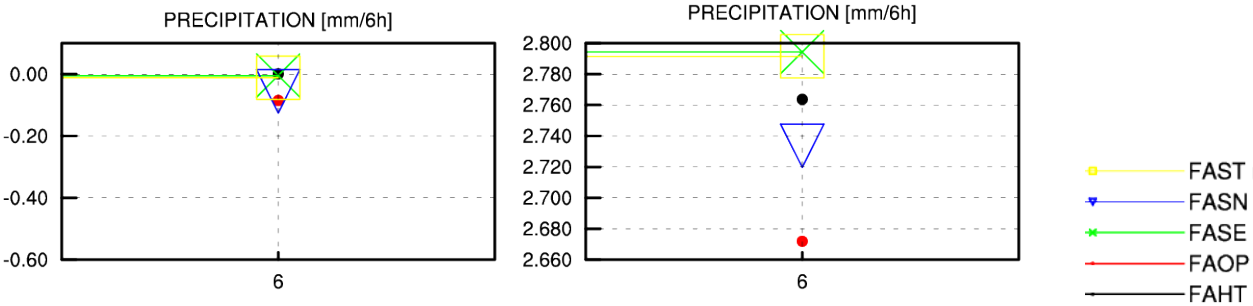


Figure 14: BIAS (left) and RMSE (right) of 6h precipitation for reference experiment AOP and radar experiments ASN, ASE, AST and AHT over the assimilation period of 20-30 June 2022 for all network times (00, 06, 12 and 18 UTC).

Fraction skill scores (FSS) were calculated for the whole period in order to evaluate precipitation fields between different experiments. Useful FSS scores [10] showed that ASE, AST and AHT experiments spatially have more accurate fields but there was some degradation for largest amounts of precipitation in experiments AST and AHT (Figure 15). As BATOR modification that sets MDRF to a fixed value per radar is present in all three of these experiments, it could imply that this change brings some benefit to the precipitation forecast.

Precipitation fields (6h accumulation) were visualised and compared with the CHMI 6h precipitation estimate (radar values adjusted with rain gauges by krieging with external drift method). Most precipitating cases showed rather similar behaviour except on the case of 20.06.2022 where all experiments behaved badly (Figure 16).

ASF and ASN exhibit the drying effect and precipitation is removed where in reality, there should be rain. But looking at the precipitating band on the south part of the Czech Republic, it is visible that ASE experiment is starting to replicate it. This band is then kept in both AST and AHT experiments. This implies the biggest positive impact (in FSS scores as well) comes from constant MDRF value.

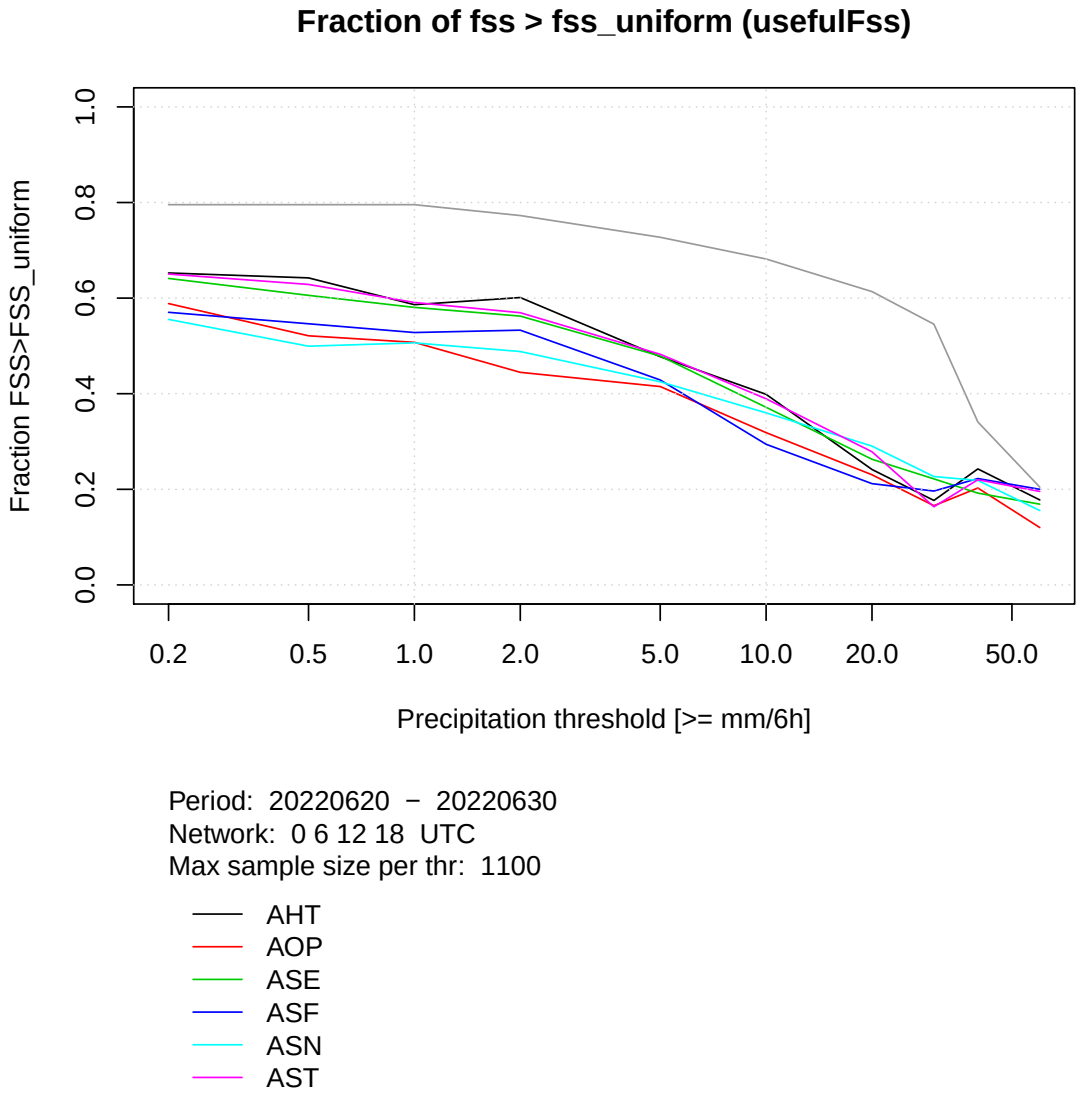


Figure 15: The fraction of forecasts which are useful (FSS > FSS_uniform). The grey line shows percentage of cases when both observed and forecasted precipitations exceed the defined threshold at least at one point.

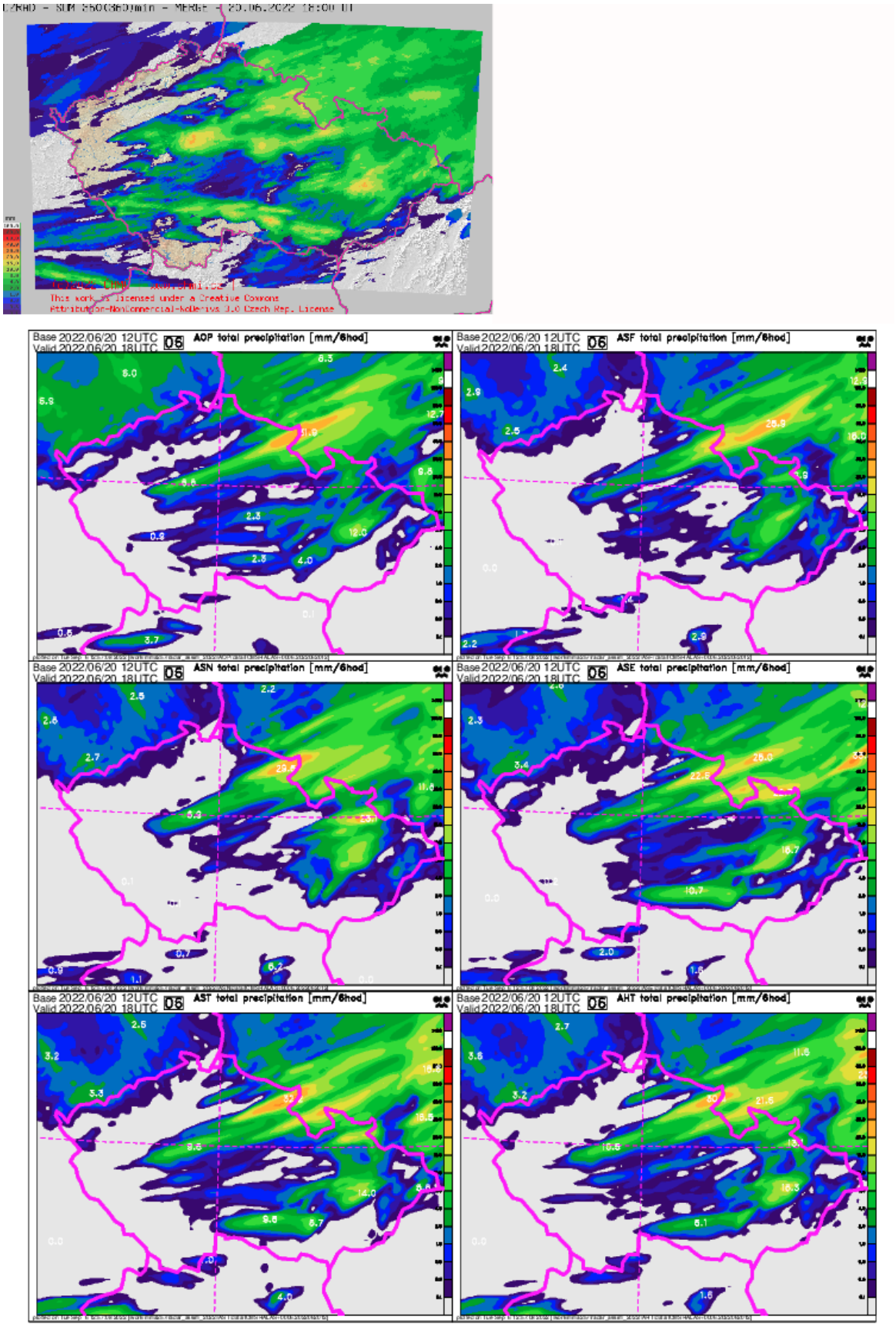


Figure 16: The 6h precipitation forecast for 20 June 2022 12UTC for lead time of +06h for experiments AOP, ASF, ASN, ASE, AST, AHT and observations – radar and rain gauges based quantitative precipitation estimate (top).

### 4.3 Varying values and distance of dry observations

Behaviour of ASE experiment prompted the need to test this sensitivity further. The Bučánek solution contains the offset of +10dBZ (Equation 2). Adding an offset to the fixed value of MDRF, when used together with MF code modification, will additionally remove some dry observations. Raising the threshold line will make it to cross the zero value at shorter distances from the radar. MF code modification will then remove all dry observations whose reflectivity value is larger than 0dBZ. This means that the radius around radar where dry observations are used in analysis will shrink. In order to test what kind of impact this distance reduction has, an experiment was set up, where the condition to remove all dry observations with reflectivity above 0dBZ has been modified. AED experiment keeps all dry observations with detection threshold values below 2dBZ.

Additionally, sensitivity to different offsets has been tested as well. AE1 experiment uses no offset, and MDRF value is a true minimum value measured at a specific radar. AE2 experiment uses an offset of +8dBZ, as opposed to ASE which uses an offset of +10dBZ. New detection threshold can be seen on Figure 17.

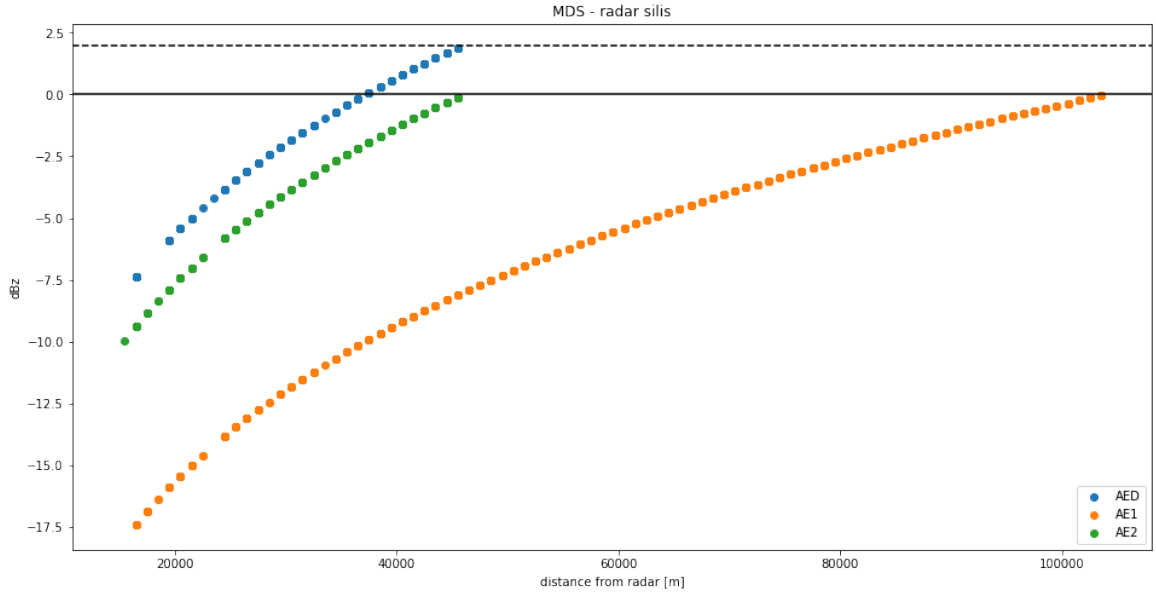


Figure 17: Detection threshold values for radar Lisca (silis) in experiments AED, AE1, and AE2.

The list of sensitivity experiments is as follows:

- ASN - default MDRF computation in BATOR & MF BATOR code modif. (>0dBZ)
- ASE - constant MDRF per radar & MF BATOR code modif. (>0dBZ) & offset = 10dBZ
- AE1 - constant MDRF per radar & MF BATOR code modif. (>0dBZ) & offset = 0dBZ
- AE2 - constant MDRF per radar & MF BATOR code modif. (>0dBZ) & offset = 8dBZ
- AED - constant MDRF per radar & MF BATOR code modif (>2dBZ) & offset = 10dBZ

Looking at the ODB statistics, it is visible that AE1 experiment with the offset of 0dBZ has stronger drying effect than the ASN experiment where BATOR is the one calculating MDRF

(Figure 18). Experiments with various positive offsets of +8dBZ and +10dBZ (AE2 and ASE) contain less observations, have larger positive reflectivity bias but smaller dry bias of pseudo-observed RH compared to the experiment with the offset of 0dBZ (AE1). So, it can be concluded that the offset helps to reduce the drying effect caused by radar data assimilation. Comparing ASE with AED (modified MF BATOR code from 0 to 2dBZ) seems to decrease RH bias.

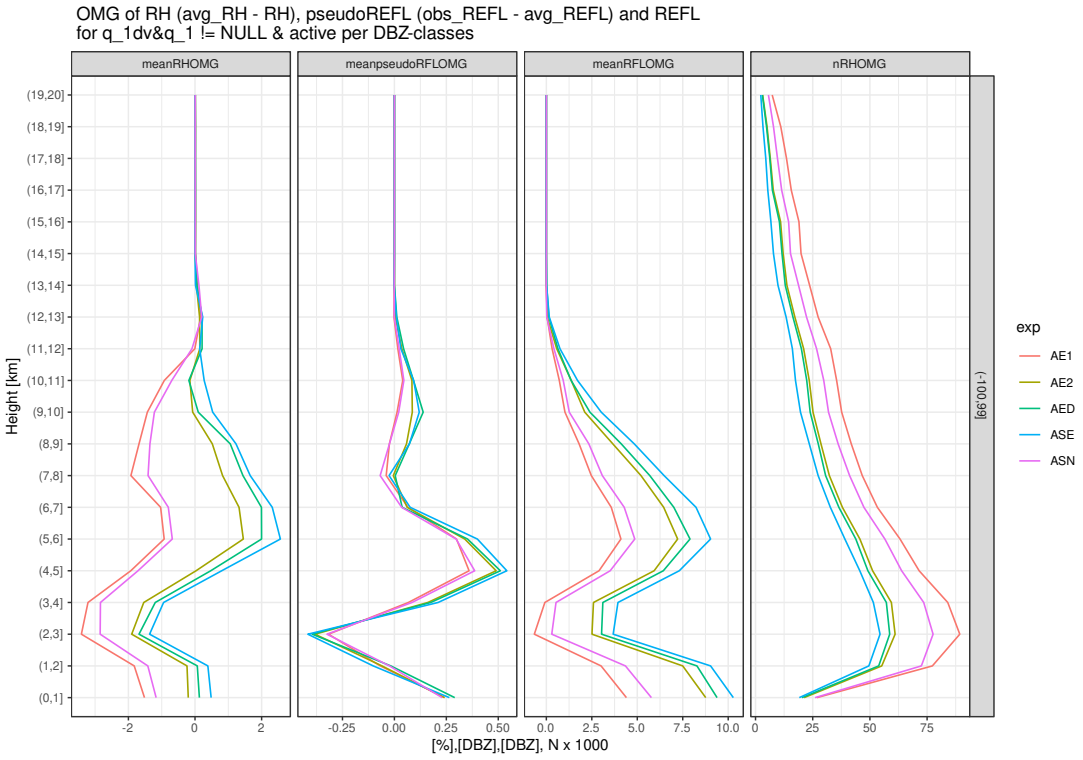


Figure 18: BIAS of departures for pseudo-observed RH, pseudo-observed reflectivity and simulated reflectivity and number of departures for ASN, ASE, AE1, AE2 and AED experiments

Both standard verification and FSS scores showed better behaviour of the ASE experiment when compared to any other experiment in this batch (example in Figure 19 and Figure 20), from which can be concluded that the positive offsets reduce drying effect and have benefits on cloudiness and precipitation forecast.

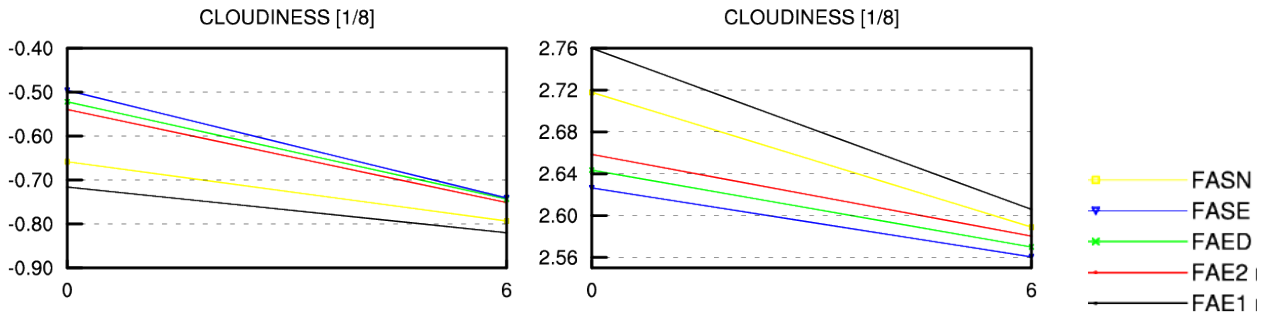


Figure 19: BIAS (left) and RMSE (right) of the cloudiness for radar experiments ASN, ASE, AE1, AE2, and AED over the assimilation period of 20-30 June 2022 for all network times (00, 06, 12 and 18 UTC).

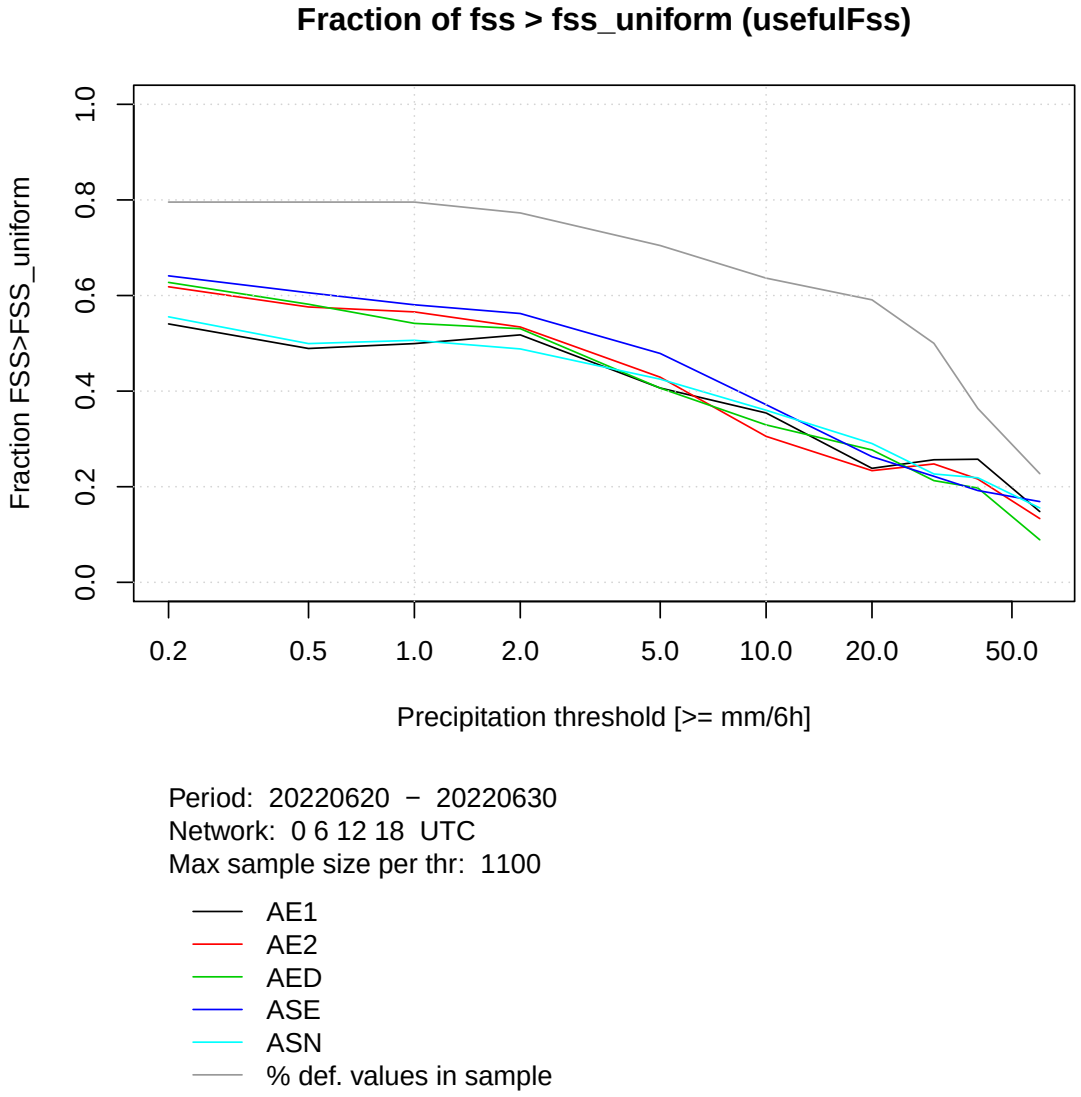


Figure 20: The fraction of forecasts which are useful (FSS > FSS_uniform). The grey line shows percentage of cases when both observed and forecasted precipitations exceed the defined threshold at least at one point.

## 4.4 Varying dry observation values depending on radar elevation

Since different radar elevations can have different values of MDRF, a smaller sample of radars was selected in order to test if multiple detection thresholds would bring some benefit. Example for Czech radar Skalky (czska) can be seen on Figure 21. The upper picture is the detection threshold with one fixed MDRF value, while lower picture shows multiple ones, depending on the elevation.

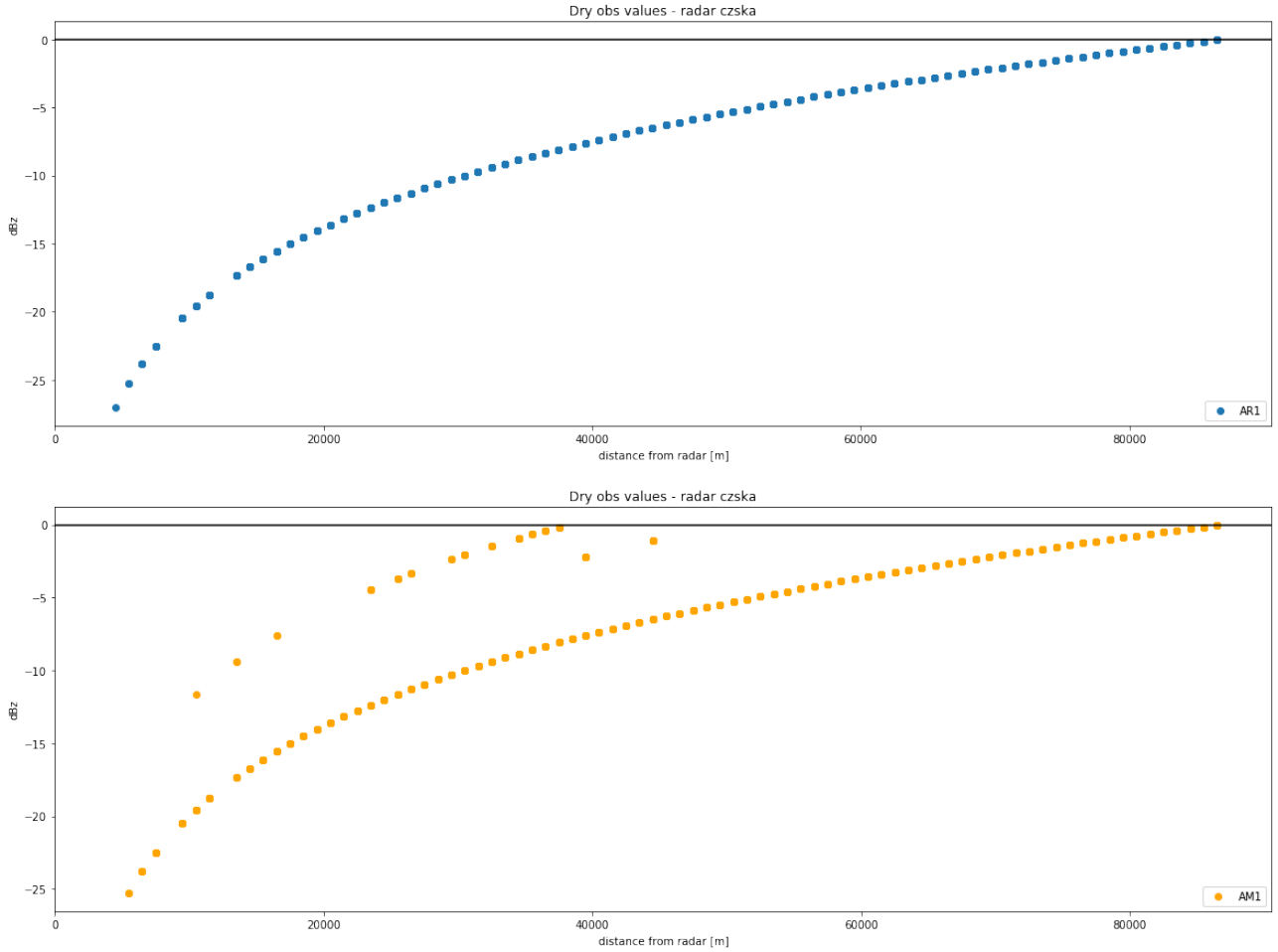


Figure 21: Detection threshold values for radar Skalky (czska) for a single constant value of MDRF (top) and MDRF values dependent on the elevation (bottom).

Dedicated set of experiments assimilated only German and Czech radars. Experiments were performed over the period 20.06.2022 - 30.06.2022.

MDRF values for all German and Czech radars were hard coded into BATOR and new experiments were set up:

- AMR - constant MDRF per radar & MF BATOR code modif. & offset = 0dBZ
- AR1 - constant MDRF per radar & MF BATOR code modif. & offset = 10dBZ
- AM0 - MDRF per elevation and radar & MF BATOR code modif. & offset = 0dBZ
- AM1 - MDRF per elevation and radar & MF BATOR code modif. & offset = 10dBZ

All scores (ODB statistics, veral, fss) showed that differences between comparable experiments (experiments with fixed MDRF value and their equivalents with variable MDRF) are rather negligible (ODB statistics in Figure 22) or mixed at best. Therefore, further development of this MDRF definition would not be sensible.

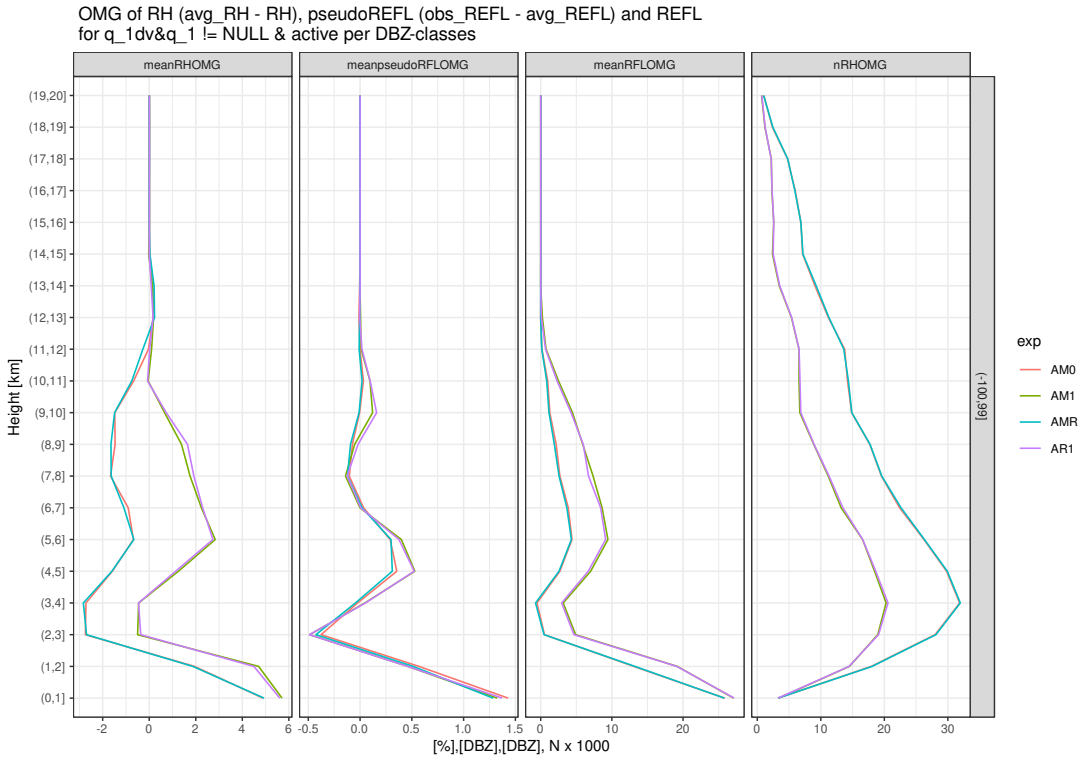


Figure 22: BIAS of departures for pseudo-observed RH, pseudo-observed reflectivity and simulated reflectivity and their count for active observations in AM0, AM1, AME, and AR1 experiments

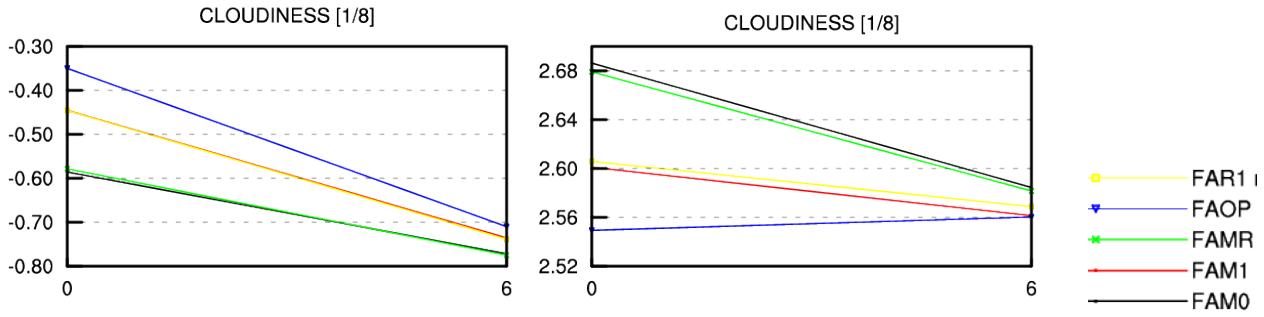


Figure 23: BIAS (left) and RMSE (right) of the cloudiness for radar experiments AOP, AMR, AM0, AM1, and AR1 over the assimilation period of 20-30 June 2022 for all network times (00, 06, 12 and 18 UTC).

## 4.5 Evaluation of Strajnar solution

In order to evaluate this solution, two experiments were set up: ASB (Strajnar solution including MDRF value fixed to true minimum value with offset of +10, same as is in ASE experiment) and ASC (Strajnar solution with default MDRF computation).

- ASN - active radar DA with default MDRF computation & MF BATOR code modif.
- ASE - active radar DA with constant MDRF per radar & MF BATOR code modifications
- ASC - as ASN & model or obs reflectivity > 12dBZ
- ASB - as ASE & model or obs reflectivity > 12dBZ

When looking at the ODB statistics it is visible that scores for both experiments (ASC and ASB) look very different when compared to any other experiment (Figure 24). The cause of such large differences is the small amount of observations that are kept in this experiment, and most of them are moist observations. This can also be seen on the histogram of active reflectivity observations at Figure 25. Since moist observations have larger discrepancies when compared to dry ones, this score is rather expected. Due to this, it would be unfair to compare them with other experiments looking at ODB statistics. But what should be highlighted is that there is a clear cut off in the ASC and ASB profiles at around 12-13 km after which no data are used in the analysis.

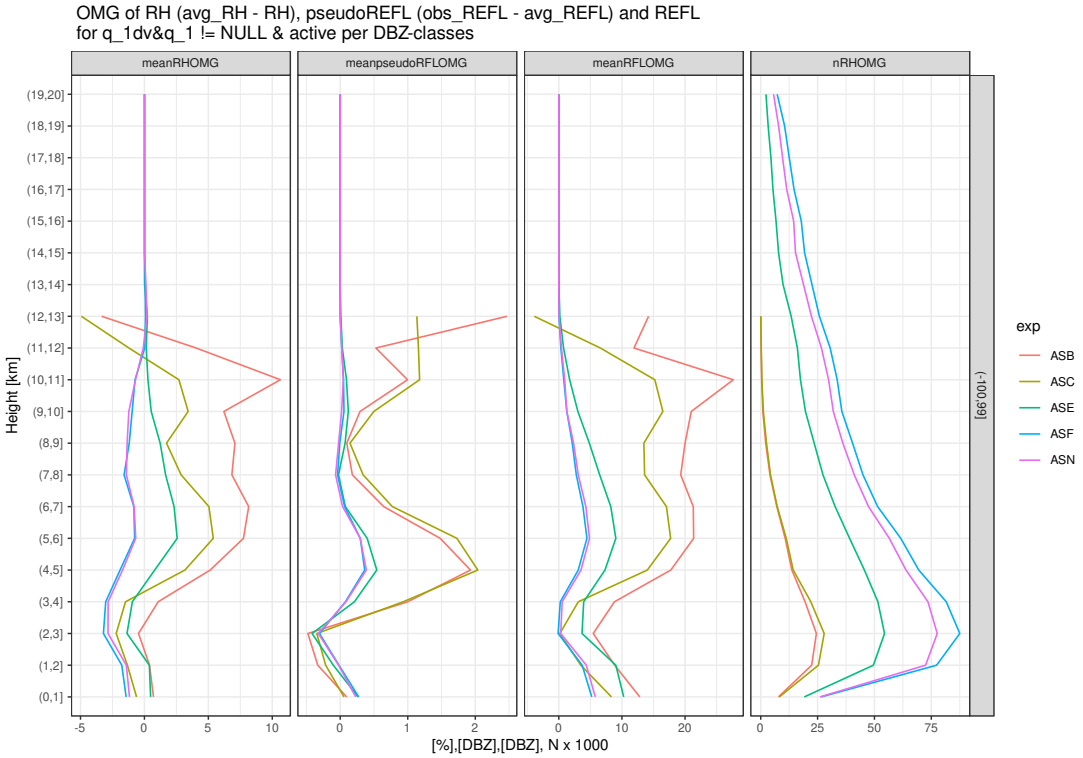


Figure 24: BIAS of departures for pseudo-observed RH, pseudo-observed reflectivity and simulated reflectivity and number of departures for ASB, ASC, ASN, ASE and ASF experiments.

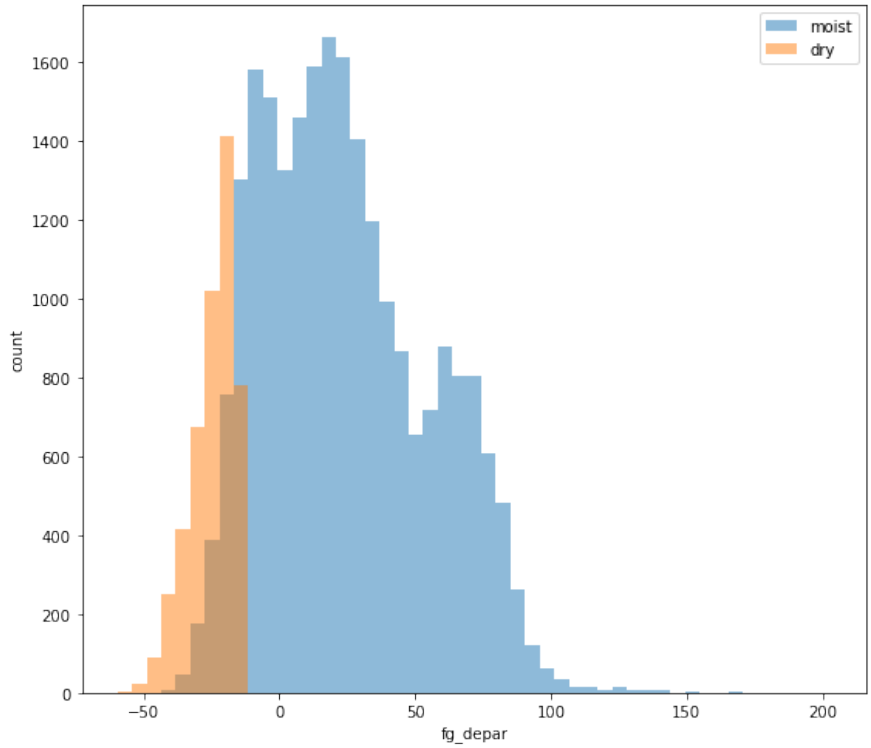


Figure 25: Histogram of first guess departures of active dry (orange) and wet (blue) reflectivity observations for experiment ASB.

Verification scores of upper-air relative humidity are fairly neutral (Figure 26). It can be seen that at the analysis time bias is slightly better for the ASB and ASC experiments compared to AOP while RMSE is neutral when compared to all other experiments. As for the 6h forecast, ASB and ASC experments have larger biases (ASB behaving slightly worse) but on the other hand RMSE for both experiments is better (ASB behaving slightly better) than the reference experiment AOP.

When considering only effect of the Strajnar solution with respect to the corresponding radar assimilation counterpart, e.g. ASC with respect to ASN, we can see that the Strajnar proposal helps to almost eliminate dry bias in 6h forecast. On the other hand when used with a fixed MDRF value (ASB vs ASE) the dry bias exists in ASB mainly between 400-600hPa. Despite that RMSE differences are very small for ASB and ASC experiments.

Verification of cloudiness (Figure 27) show that ASB and ASC experiments help to almost eliminate negative bias of cloudiness and ASB even outperforms the reference experiment AOP.

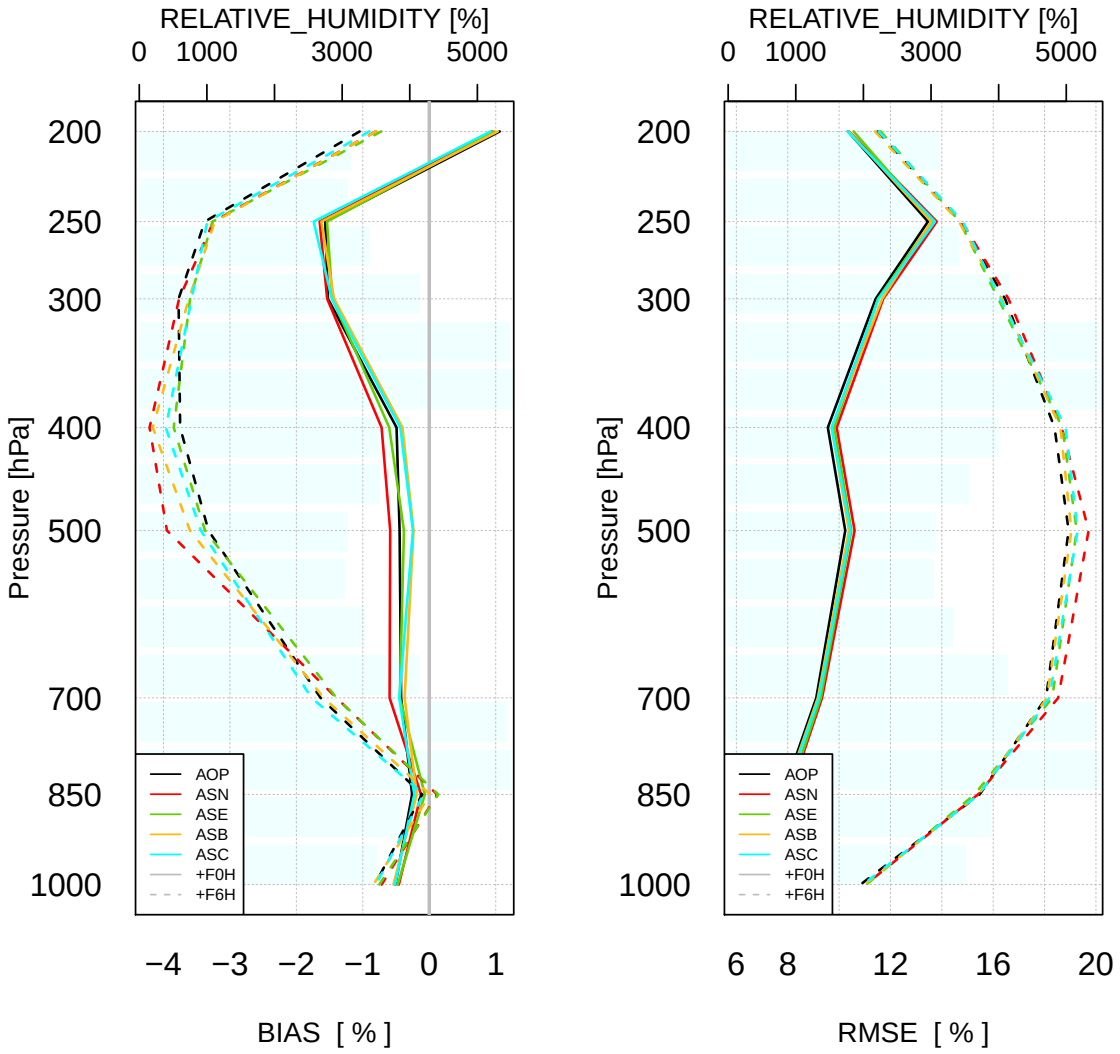


Figure 26: BIAS (left) and RMSE (right) of relative humidity for reference experiment AOP and radar experiments ASN, ASE, ASB and ASC over the assimilation period of 20-30 June 2022 for all network times (00, 06, 12 and 18 UTC).

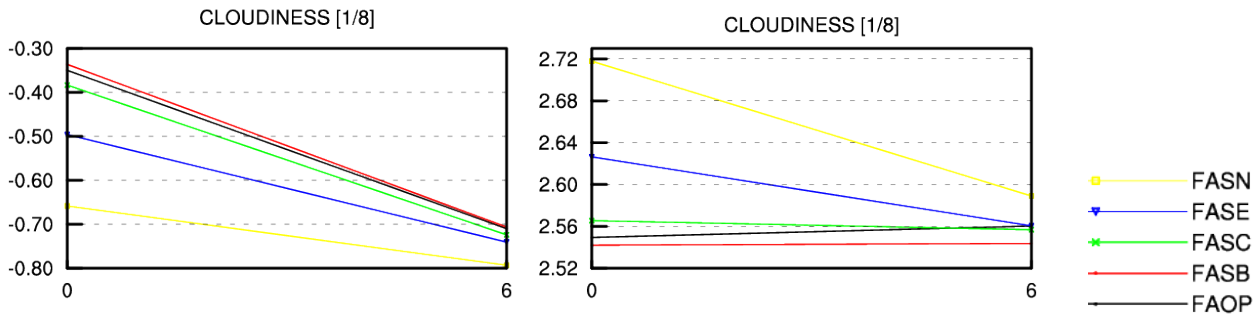


Figure 27: BIAS (left) and RMSE (right) of the cloudiness for reference experiment AOP and for radar experiments ASN, ASE, ASB, and ASC over the assimilation period of 20-30 June 2022 for all network times (00, 06, 12 and 18 UTC).

Looking at the useful FSS scores, it can be seen that a fixed MDRF value (ASE experiment) performs the best and it's addition brings some benefit to the Strajnar solution as well (Figure 28).

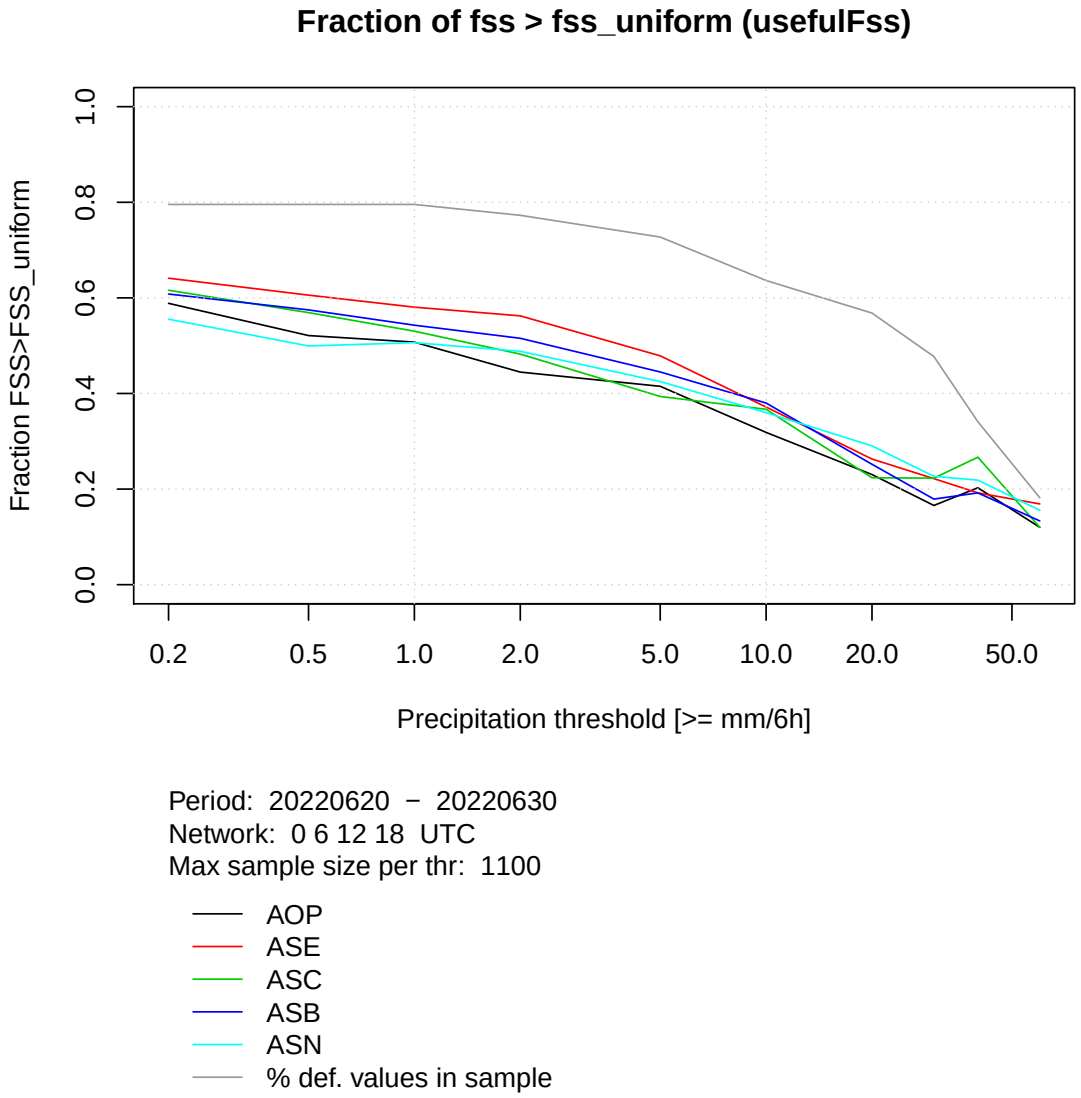


Figure 28: The fraction of forecasts which are useful (FSS > FSS_uniform). The grey line shows percentage of cases when both observed and forecasted precipitations exceed the defined threshold at least at one point.

If precipitation fields for the 20.06.2022 12 UTC case are compared (Figure 29), it can be seen that ASB experiment (lower right) has less drying where there should be no drying. Unfortunately, in ASC and ASB experiments the band at south of the Czech Republic is no longer there (as was in ASE experiment).

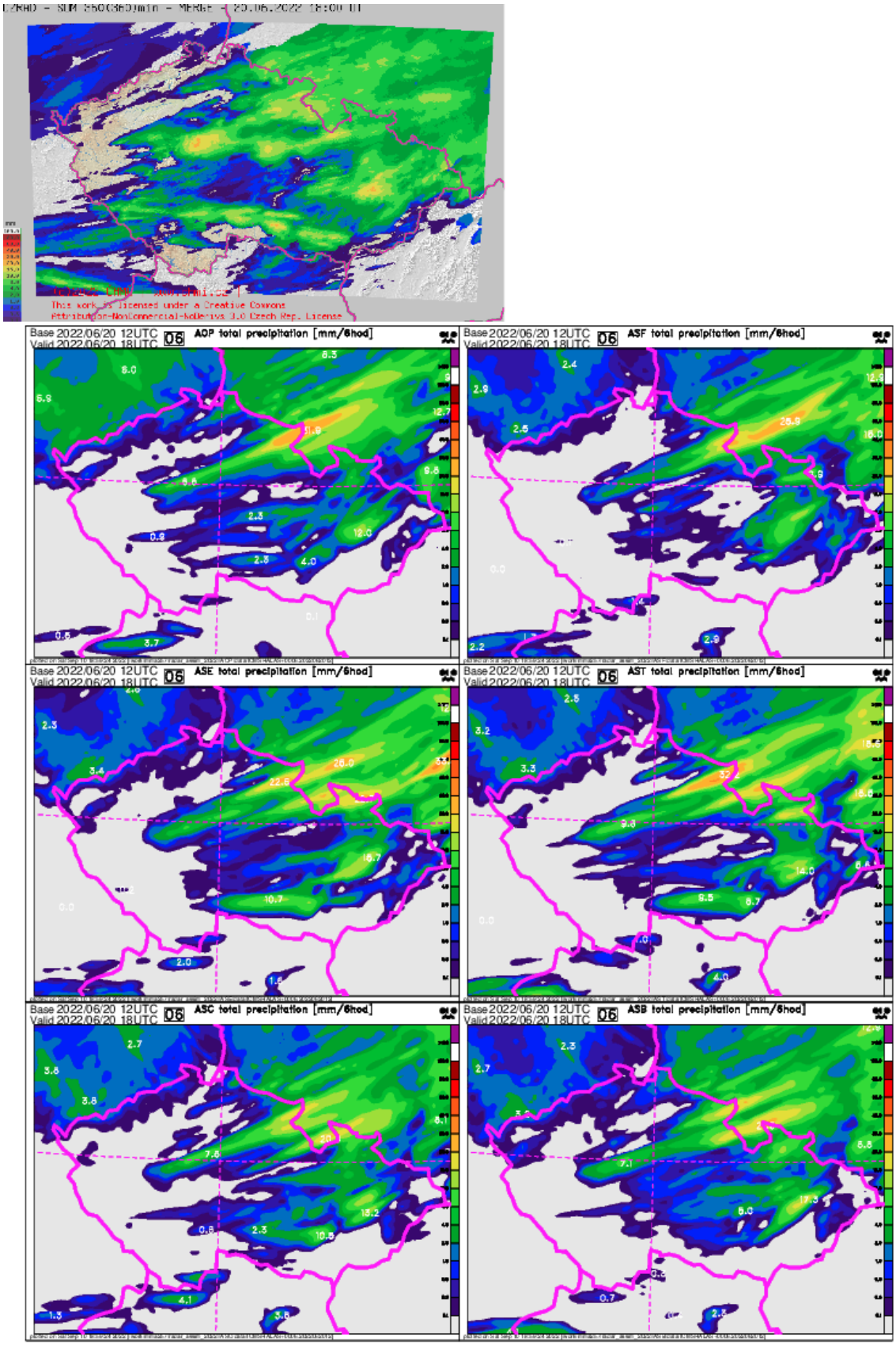


Figure 29: The 6h precipitation forecast for 20 June 2022 12UTC for lead time of +06h for experiments AOP, ASF, ASE, AST, ASC, ASB and observations – radar and rain gauges based quantitative precipitation estimate (top).

# 5 Conclusions

The aim of this study was to evaluate an impact of the two proposals to suppress drying effect which has been observed during assimilation of radar reflectivity in ALARO CMC (Panežić et al 2021).

The first proposal by Bučánek contained two modifications: the constant MDRF (per radar with additional offset of 10dBZ) and the removal of dry observations that are moistening the atmosphere. The first setting of the constant MDRF removed the dry bias in upper-air relative humidity, helped to mitigate negative bias in cloudiness and improved the useful FSS precipitation scores. The combination of the constant MDRF with the removal of dry observation that are moistening the atmosphere showed pronounced drying in the higher atmosphere due to the existence of only dry observations at such altitudes. The additional removal of very high dry observations showed that different non-optimal profiles might be selected during the screening process, which might degrade the forecast.

Results showed large sensitivity to MDRF and offset which define values applied to dry observations. Adding a positive offset improved the forecast of precipitation and relative humidity, reducing the drying effect. Testing different MDRF values depending on elevation showed very small impact so it would not be sensible to continue the research in this direction.

The second proposal by Strajnar suggests to assimilate only the observations where there is reflectivity above 12 dBZ in either the model or observations. This approach eliminates a lot of observations. However, even with a very small number of data, it provides good results.

This proposal was tested with and without a constant MDRF value. In combination with a constant MDRF value, the Strajnar proposal (ASB) mitigated the dry bias in upper-air relative humidity and outperformed scores in cloudiness with respect to the reference AOP. In the standalone Strajnar solution (ASC) the improvements in upper-air relative humidity and cloudiness are less pronounced but still fairly comparable with the reference AOP. The useful FSS scores showed some benefit of Strajnar proposal in the combination with a constant MDRF value.

# References

[1] https://www.eumetnet.eu/activities/observations-programme/current-activities/opera/

[2] Olivier Caumont, Véronique Ducrocq, Éric Wattrelot, Geneviéve Jaubert and Stéphanie Pradier-Vabre; *1D+3DVar assimilation of radar reflectivity data: a proof of concept;* Tellus A: Dynamic Meteorology and Oceanography, vol. 62, issue 2, pp. 173-187, 2010.

[3] Éric Wattrelot, Olivier Caumont, and Jean-François Mahfouf; *Operational Implementation of the 1D+3D-Var Assimilation Method of Radar Reflectivity Data in the AROME Model;* Monthly Weather Review, vol. 142, issue 5, pp. 1852–1873 , 2014.

[4] Antonín Bučánek; *Processing of radar reflectivities in screening;* 2020., 10 pp

[5] Alena Trojáková; *ALARO tests of radar observation operator;* 2020., 16 pp

[6] Suzana Panežić, Alena Trojáková, and Antonín Bučánek; *Impact studies with OPERA reflectivity observations;* 2021., 26 pp

[7] Benedikt Strajnar; *(2022, April 6th) Data Assimilation Session: Overview of LACE DA activities;* 2nd ACCORD ASW, Ljubljana

[8] Antonín Bučánek; *(2022, April 6th) Data Assimilation Session: Progress on reflectivity DA at CHMI;* 2nd ACCORD ASW, Ljubljana

[9] Merril I. Skolnik; *Radar handbook;* 2nd edition; 1990; McGraw-Hill, Inc.

[10] Zacharov, Řezáčová 2019: The verification of the QPF produced by ALADIN-CZ model, Meteorolické zprávy

# Appendix A: Experiments - BATOR setup

| EXP | LREADMDS | LREADMDSMOD | LNOISEDISTRED | ZRADOFFSET | ZNULTHRVAL |
|---|---|---|---|---|---|
| AOP | | | | | |
| NSF | F | F | F | 0 | 0 |
| NSN | F | F | T | 0 | 0 |
| NSE | T | F | T | 0 | 0 |
| NST | T | F | T | 0 | 0 |
| NSB | T | F | T | 0 | 0 |
| ASF | F | F | F | 0 | 0 |
| ASN | F | F | T | 0 | 0 |
| ASE | T | F | T | 0 | 0 |
| AE1 | T | F | T | -10 | 0 |
| AE2 | T | F | T | -2 | 0 |
| AED | T | F | T | 0 | +2 |
| AST | T | F | T | 0 | 0 |
| AHT | T | F | T | 0 | 0 |
| ASB | T | F | T | 0 | 0 |
| ASC | F | F | T | 0 | 0 |
| AMR | F | F | T | 0 | 0 |
| AM0 | F | T | T | 0 | 0 |
| AR1 | F | F | T | +10 | 0 |
| AM1 | F | T | T | +10 | 0 |
| AME | F | T | T | +5 | 2 |

Table 1: Summary of experiments - BATOR setup.

# Appendix B: Experiments - model setup

| EXP | LRAINTHR | LRMDRYOBSMOIST | ZRAINTHRVAL | LMAXHEIGHT10KM |
|---|---|---|---|---|
| AOP | | | | |
| NSF | F | F | 0 | F |
| NSN | F | F | 0 | F |
| NSE | F | F | 0 | F |
| NST | F | T | 0 | F |
| NSB | T | F | 12 | F |
| ASF | F | F | 0 | F |
| ASN | F | F | 0 | F |
| ASE | F | F | 0 | F |
| AE1 | F | F | 0 | F |
| AE2 | F | F | 0 | F |
| AED | F | F | 0 | F |
| AST | F | T | 0 | F |
| AHT | F | T | 0 | T |
| ASB | T | F | 12 | F |
| ASC | T | F | 12 | F |
| AMR | F | F | 0 | F |
| AM0 | F | F | 0 | F |
| AR1 | F | F | 0 | F |
| AM1 | F | F | 0 | F |
| AME | F | F | 0 | F |

Table 2: Summary of experiments - model setup.

# Appendix C: Technical details

## C.1 Source code modifications

Executables were based on the local model release CY43t2ag_op1. The modified sources can be found on kazi:

`/work/mma257/radar_assim_2022/build_CY43t2ag_op1radar_ab_bs`

## C.2 Experiments

Scripts and namelists related to all experiments can be found on kazi:

`/home/mma257/radar_assim_2022`

Results are stored on archive in directory:

`~mma257/exp/`